

# A semi-analytical equation for the Young's modulus of isotropic ceramic materials

Dionissios T. Hristopoulos<sup>a,\*</sup>, Melina Demertzi<sup>b,c</sup>

<sup>a</sup> Department of Mineral Resources Engineering, Technical University of Crete, Chania 73100, Greece

<sup>b</sup> Department of Electronic and Computer Engineering, Technical University of Crete, Chania 73100, Greece

Received 25 April 2007; received in revised form 5 September 2007; accepted 12 October 2007

## Abstract

This paper proposes a new relation between the Young's modulus of ceramics and the volume fraction of porosity. The relation is obtained by *upscaling* (coarse-graining) the fluctuations of the microstructure. The microstructure is modeled in terms of phase random fields, which upon upscaling lead to elastic coefficients described by continuous spatial random fields. The effective (macroscopic) elastic modulus is then obtained by averaging over the continuum-scale disorder. Using physically motivated arguments, an explicit expression between the Young's modulus and the porosity is proposed. This expression involves three empirical parameters, i.e. the solid-phase modulus and two perturbation coefficients. The parametric expression is shown to fit well experimental measurements from the literature. Empirical "bounds" for the Young's modulus are also formulated. These bounds account for variations due to microstructural properties that are not explicitly calculated in the upscaling.

© 2007 Elsevier Ltd. All rights reserved.

PACS: 81.07.Bc; 81.10.Aj; 81.20.Ev

Keywords: C. Mechanical properties; B. Porosity; B. Microstructure-final

## 1. Introduction

The structure of ceramic materials is heterogeneous due to variations in the porosity, composition and mass density. The local structure variations lead to subsequent variations in the mechanical properties. For engineering purposes, it is desirable to relate explicitly the structural and mechanical properties, e.g. by means of constitutive relations between the local elastic properties and the porosity<sup>1</sup>. In the case of isotropic ceramics the elastic coefficients are determined from the Young's modulus and the Poisson's ratio.<sup>2</sup> The present study focuses on the porosity dependence of the Young's modulus measured at constant temperature. Studies on the temperature dependence of the Young's modulus suggest a linear relation, e.g.<sup>3</sup>

In the case of materials with spatially non-uniform properties, the macroscopic elastic behavior is determined from the coarse-grained elastic moduli that relate the *average* stress and deformation tensors. Various approximate theories for the estimation of the Young's modulus have been formulated that link its value to the porosity of ceramics, e.g.<sup>3,4</sup> A number of these models are reviewed and evaluated in<sup>5</sup>. A more recent, critical review of the most commonly used modulus–porosity relations is found in<sup>6</sup>.

In a recent paper<sup>1</sup> the Young's modulus and Poisson's ratio for model ceramics, generated by computer simulations, were investigated. The Finite Element Method was used to determine the local deformations resulting from imposed stress and thus to obtain estimates of the effective elastic moduli as a function of the porosity. The estimates were subsequently corrected for finite-size effects. Then, the estimated moduli were fitted to the Phani–Niyogi expression,<sup>7</sup> i.e.  $E_{\text{eff}} = E_s(1 - \phi/\phi_0)^n$ , where  $E_s$  represents the elastic modulus of the solid phase and  $\phi_0$  the percolation threshold. The empirical parameters  $\phi_0 \approx 0.652$  and  $n \approx 2.23$  were determined by numerically fitting the model curve of  $E_{\text{eff}}$  versus  $\phi$  to the synthetic data. This expression led to better agreement with published data than

\* Corresponding author.

E-mail address: [dionisi@mred.tuc.gr](mailto:dionisi@mred.tuc.gr) (D.T. Hristopoulos).

URL: <http://www.mred.tuc.gr/home/hristopoulos/dionisi.html>

(D.T. Hristopoulos).

<sup>c</sup> Present address: Department of Computer Science, University of Southern California, USA.

estimates based on three different microstructure models (overlapping spheres, overlapping spherical pores and overlapping ellipsoidal pores). The Phani–Niyogi expression for the Young's modulus is independent of the Poisson's ratio, a property that in practice holds for ceramic materials with porosities up to 0.4. This relation interpolates smoothly between  $E_{\text{eff}} = E_s$  at zero porosity to  $E_{\text{eff}} = 0$  at the percolation threshold. However, to our knowledge there is no physical motivation for the power-law dependence of this equation, and in particular for the non-integer value of the exponent. The values of the fit parameters  $\phi_0$  and  $n$  are not universal but depend on the type of the ceramics and the microstructure obtained (thus on the preparation method); for example, this can be seen by comparing the parameter values obtained in <sup>1</sup> with the respective values (Table 3) in <sup>6</sup>.

The conceptual model presented here focuses on two-phase, isotropic and “ideal ceramics”. It assumes that the elastic properties are determined purely from the microstructure and not from elastic defects (i.e. micro-cracks), that may be independent from the geometry of the pore space. The experimentally measurable Young's modulus is obtained by coarse-graining the microstructure, leading to a perturbation expansion in terms of the volume fraction of porosity.<sup>d</sup> A physical argument is then used to include the impact of defects in the coefficients of the perturbation expansion. The resulting expansion uses  $\bar{\phi}/(1 - \bar{\phi})$ , where  $\bar{\phi}$  is the mean volume fraction of porosity, as the series expansion parameter. In this respect it differs from other analytical expressions. The physical meaning of this expansion is discussed in the following sections. Finally, the model applies to materials with porosity in the range 0–0.4, which is representative for most ceramics.

## 2. Conceptual model of structure – elasticity relations

The conceptual model of ceramic structure proposed here connects three different scales, which will be referred to as the micro, the local and the macro scales. At the micro scale the structure is determined by the binary phase field that distinguishes between solid and pore space, and the variations of the solid phase modulus. At the local scale the variations of the elastic coefficients are assumed to be continuous. The macro scale corresponds to the size of the experimental samples, which is assumed large enough to allow averaging over the local variations.

Let  $\mathbf{s}$  denote any point inside the ceramic material. In the micro scale representation, the elastic modulus will be denoted by  $E(\mathbf{s})$ , at the local scale by  $E(\mathbf{s}; \ell)$  where  $\ell$  is the reference local scale; at the macro scale  $E_{\text{eff}}$  will be used to denote the effective elastic modulus. The final result at the macro scale is an expression for the elastic modulus that depends on the volume fraction of porosity. The expression involves two empirical coefficients that incorporate properties specific to the microstructure of the ceramic material.

<sup>d</sup> Note that the term coarse-graining is used herein to denote the mathematical procedure of obtaining a physical model under a change-of-scale transformation (upscaling), and it is not linked to a particular grain size.

### 2.1. Micro scale: phase field representation

The microstructure of ceramic materials is determined by the irregular distribution of the locations, sizes and shapes of the pores as well as the spatial distribution of the constituent material phases. Thus the structure can be described by means of a stochastic model that allows for randomly correlated variations. Stochastic models of the microstructure are common in porous media research.<sup>4,8</sup> Stochastic methods have also been developed for reconstructing the microstructure from partial information (e.g. tomographic slices).<sup>9–11</sup>

In the following, *ensemble averages* (i.e. expected values) over the fluctuations (disorder) of the microstructure will be denoted<sup>e</sup> by  $\mathbb{E}[\cdot]$ . For brevity, the horizontal bar will be used to denote single-point expectations (mean values).

#### 2.1.1. The phase field

In the case of two-phase media, the pore space can be distinguished from the solid matrix in terms of the binary *phase random field*  $\chi(\mathbf{s})$ , which takes values  $\chi(\mathbf{s}) = 1$  in the solid and  $\chi(\mathbf{s}) = 0$  in the pore space. The mean value and variance of the phase field are given by  $\mathbb{E}[\chi(\mathbf{s})] \equiv \bar{\chi} = 1 - \bar{\phi}$ , where  $\bar{\phi} = \mathbb{E}[\phi(\mathbf{s})]$  is the *mean volume porosity* (volume fraction of porosity). Similarly, the phase field variance is given by  $\sigma_\chi^2 = \bar{\phi}(1 - \bar{\phi})$ .

Let  $\chi'(\mathbf{s}) = \chi(\mathbf{s}) - \bar{\chi}$  denote the fluctuation of the phase field. The phase-field *two-point correlation function* between any two points  $\mathbf{s}_1$  and  $\mathbf{s}_2$  inside the ceramic material is given by  $c_\chi(\mathbf{s}_1 - \mathbf{s}_2) = \mathbb{E}[\chi'(\mathbf{s}_1)\chi'(\mathbf{s}_2)]$ . Higher-order (multipoint) correlation functions can also be defined, and they incorporate higher-order information about the microstructure [4, Chapter 2]. For isotropic materials the correlation function's main parameter is the correlation length,  $\xi_0$ , which determines the range of spatial dependence (in the statistical sense). The functional form of the correlation function embodies additional information about the microstructure. The variability of the structure is determined from the phase-field coefficient of variation, i.e.

$$\mu_\chi^2 = \frac{\sigma_\chi^2}{\bar{\chi}^2} = \frac{\bar{\phi}}{1 - \bar{\phi}}. \quad (1)$$

It follows from Eq. (1) that  $\mu_\chi^2$  increases monotonically with  $\bar{\phi}$ . For example,  $\mu_\chi \approx 0.11$  for  $\bar{\phi} = 0.1$ , while  $\mu_\chi \approx 0.67$  for  $\bar{\phi} = 0.4$ . Hence, the variability is small for values of  $\bar{\phi} \approx 0$ , while  $\mu_\chi \rightarrow 1$  as  $\bar{\phi} \rightarrow 0.5$ . This observation suggests that low-porosity materials can be modeled by means of low-order perturbation expansions around the uniform solid phase ( $\bar{\phi} = 0$ ).

Complete knowledge of the microstructure requires the joint (multi-point) probability density function of  $\chi(\mathbf{s})$  [4, pp. 23–58]. This is very difficult in practice, since from experimental samples one can determine at best low-order correlation functions, which permit a partial reconstruction of the microstructure [4, pp. 269–302]. However, a low-order characterization of the microstructure should suffice for deriving approximate values

<sup>e</sup> From a mathematical/operational perspective,  $\mathbb{E}[\cdot]$  denotes the *expectation* over the probability distribution of the fluctuations.

of the elastic properties of ceramics, if  $\bar{\phi}$  is less than 0.5. In the following, we focus on this *weak heterogeneity* limit, and in particular on  $\bar{\phi} < 0.4$ . In this limit, it is justified to ignore the products of fluctuations, which represent small quantities.

### 2.1.2. The elastic modulus: homogeneous solid phase

Let the elastic modulus of the solid phase be denoted by  $E_s$ . If variations in  $E_s$  are ignored, the micro-scale modulus is given by  $E(\mathbf{s}) = E_s \chi(\mathbf{s})$ . This assumption is reasonable for two-phase, ideal ceramics. Consequently, the mean value of the elastic modulus characterizing the porous medium at this scale is given by:

$$\mathbb{E}[E(\mathbf{s})] = \overline{E(\mathbf{s})} = E_s(1 - \bar{\phi}), \quad (2)$$

and the variance by

$$\sigma_E^2 = E_s^2 \sigma_\chi^2 = E_s^2 \bar{\phi}(1 - \bar{\phi}). \quad (3)$$

Hence, the coefficient of variation of the elastic modulus is controlled by the phase field, i.e.  $\mu_E \equiv \sigma_E / \bar{E} = \mu_\chi$ .

### 2.1.3. The elastic modulus: non-homogeneous solid phase

If variations in the elastic modulus of the solid matrix are considered, e.g. due to the presence of more than one phases or elastic defects, then  $E_s$  should be replaced by the random field  $E_s(\mathbf{s})$ . Then, the local elastic modulus is given by:

$$E(\mathbf{s}) = E_s(\mathbf{s}) \chi(\mathbf{s}). \quad (4)$$

The phase field may be *spatially uncorrelated* with  $E_s(\mathbf{s})$ ; this is a justifiable assumption, since the former relates to the distribution of pores in the microstructure, while the latter relates to variations of the solid modulus, given that the specific point is in the solid phase. To avoid confusion it is emphasized that the local modulus  $E(\mathbf{s})$  is always correlated with the phase field  $\chi(\mathbf{s})$ , as it follows from Eq. (4). Let us decompose the solid phase modulus into a mean value and a fluctuation, i.e.  $E_s(\mathbf{s}) = \bar{E}_s + E'_s(\mathbf{s})$ ; the variance of the solid phase modulus fluctuations is denoted by  $\text{Var}(E_s)$  and the coefficient of variation by  $\mu_{E_s}$ . Then, in light of Eq. (4), the local modulus is expressed as follows:

$$E(\mathbf{s}) = \bar{E}_s(1 - \bar{\phi}) + E'_s(\mathbf{s})(1 - \bar{\phi}) + \chi'(\mathbf{s})\bar{E}_s + \chi'(\mathbf{s})E'_s(\mathbf{s}). \quad (5)$$

In the weak heterogeneity limit, the term  $\chi'(\mathbf{s})E'_s(\mathbf{s})$  is negligible, since it involves a product of two fluctuations. In the following, we consider only terms that are linear in the fluctuations. This means that the mean modulus is given by:

$$\mathbb{E}[E(\mathbf{s})] = \bar{E}_s(1 - \bar{\phi}). \quad (6)$$

It follows from the Eqs. (5) and (6) that the fluctuation of the elastic modulus is given by:

$$E'(\mathbf{s}) = E'_s(\mathbf{s})(1 - \bar{\phi}) + \chi'(\mathbf{s})\bar{E}_s. \quad (7)$$

Using the definition  $\text{Var}(E_s) = \mathbb{E}[E_s'^2(\mathbf{s})]$ , based on Eq. (7) the variance of the modulus is given by:

$$\begin{aligned} \sigma_E^2 = & \text{Var}(E_s)(1 - \bar{\phi})^2 + \bar{E}_s^2(1 - \bar{\phi})\bar{\phi} \\ & + 2\bar{E}_s(1 - \bar{\phi})\mathbb{E}[\chi'(\mathbf{s})E'_s(\mathbf{s})]. \end{aligned} \quad (8)$$

In deriving Eq. (8) we used the linear property of the expectation, i.e. if  $a$  is a constant and  $X$  a random variable, then  $\mathbb{E}[aX] = a\mathbb{E}[X]$ . The third term in Eq. (8) is proportional to the expectation of a fluctuation product which is negligible in the weak-heterogeneity limit. Hence, the most significant contributions to  $\sigma_E^2$  come from the first two terms on the right hand side of Eq. (8), and the third term can be dropped.

In light of Eqs. (6) and (8), the coefficient of variation of the elastic modulus is increased by the coefficient of variation of the solid-phase modulus, and it is given by:

$$\mu_E^2 = \mu_{E_s}^2 + \mu_\chi^2 = \mu_{E_s}^2 + \bar{\phi}/(1 - \bar{\phi}). \quad (9)$$

If the variability of the solid-phase modulus is related to elastic defects, it is reasonable to postulate a relation between the porosity and  $\mu_{E_s}$ , since a higher probability of defects can be expected for a larger specific interfacial area between pore space and solid matrix of the ceramic. We assume a *proportional effect* of the microstructure on the variability of the solid-phase modulus, i.e.  $\mu_{E_s}^2 = \alpha\mu_\chi^2$ , where  $\alpha$  is a constant, not necessarily small. In particular, the effect of cracks can be incorporated in  $\alpha$ . In light of this hypothesis it follows that:

$$\mu_E^2 = (1 + \alpha)\mu_\chi^2. \quad (10)$$

The above hypothesis is not as obvious if the variability of the solid-phase modulus is due to the presence of more than one solid phases. For multi-phase ceramics, the variability of the solid-phase modulus will include a contribution that is independent of the porosity. Note that if we neglect the variability of the solid-phase modulus, then  $\alpha = 0$  and the coefficient of variation is reduced to the expression for the homogeneous solid phase.

## 2.2. Local scale: continuum elastic modulus

At the micro scale the variations of the elastic modulus are discontinuous, due to the binary phase field that changes between the values zero and one. At the continuum scale, which will be denoted by  $\ell$ , it is assumed that the elastic modulus variations are differentiable and the classical (continuum) theory of elasticity holds.<sup>2</sup> This is due to the smoothing effect of the coarse-graining. The values of the elastic moduli are obtained from a coarse-graining of the micro-scale values over a representative elementary volume (REV), i.e. a sphere of radius  $\ell$ .<sup>12</sup>

### 2.2.1. Coarse-graining the phase field

Coarse-graining of the microstructure leads to a local phase field  $\chi(\mathbf{s}; \ell) = V_\ell^{-1} \int \text{ds}' \chi(\mathbf{s} + \mathbf{s}')$ , where  $V_\ell$  is the volume of the radius- $\ell$  sphere centered at  $\mathbf{s}$ ,  $\mathbf{s} + \mathbf{s}'$  denotes a vector whose center is at the point  $\mathbf{s}$  and the end point is inside  $V_\ell$ , and  $\int \text{ds}'$  denotes the volume integral over all the vectors  $\mathbf{s}'$  such that the points  $\mathbf{s} + \mathbf{s}'$  are inside  $V_\ell$ . Essentially, this operation replaces the phase field at each point by the average of the field values in the local neighborhood  $V_\ell$ . The coarse-grained phase field forms the basis of the local porosity theory.<sup>13,14</sup> Since the REV contains a large number of point values (albeit spatially correlated), the central limit theorem suggests that the coarse-grained phase field tends to follow the Gaussian distribution.<sup>15</sup>

The mean value of the phase field remains unchanged by the linear coarse-graining transformation, i.e.  $\mathbb{E}[\chi(\mathbf{s}; \ell)] = \bar{\chi}$  and  $\mathbb{E}[\phi(\mathbf{s}; \ell)] = \bar{\phi}$ . However, both the variance  $\sigma_\chi^2(\ell)$ , and the correlation length  $\xi_\ell$ , of the phase field are affected by the coarse-graining. More specifically, the local phase field variance  $\sigma_\chi^2(\ell) = \text{Var}[\chi(\mathbf{s}; \ell)]$  is reduced by coarse-graining<sup>16</sup> as follows:

$$\sigma_\chi^2(\ell) = g_\ell \bar{\phi}(1 - \bar{\phi}), \quad (11)$$

where  $g_\ell < 1$ . The constant  $g_\ell$  depends primarily on the ratio  $\ell/\xi_0$  and secondarily on the specific form of the microstructure correlation function  $c_\chi(\mathbf{r})$ .

The coarse-graining scale  $\ell$  should be sufficiently large for the continuum assumption to be valid, i.e. for the phase field to change smoothly over distances of order  $\ell$ . Roughly speaking, this requires the condition  $\mathbb{E}[\chi(\mathbf{s}; \ell)]/\|\nabla\mathbb{E}[\chi(\mathbf{s}; \ell)]\| > \ell$ . Since the magnitude of the phase field's slope is on average determined from the correlation length, this condition corresponds to  $\xi_\ell > \ell$ .

### 2.2.2. Coarse-graining the elastic modulus

At the local scale, it is assumed that the elastic modulus is given approximately by  $E(\mathbf{s}; \ell) = E_s(\mathbf{s}; \ell) \chi(\mathbf{s}; \ell)$ . This is based on the following arguments: The coarse-grained solid-phase elastic modulus is defined by:

$$E_s(\mathbf{s}; \ell) = V_\ell^{-1} \int d\mathbf{s}' E_s(\mathbf{s} + \mathbf{s}'). \quad (12)$$

The coarse-grained elastic modulus is defined as:

$$E(\mathbf{s}; \ell) = V_\ell^{-1} \int d\mathbf{s}' E_s(\mathbf{s} + \mathbf{s}') \chi(\mathbf{s} + \mathbf{s}').$$

Using the mean value theorem [17, p. 379] the above is expressed as follows:

$$E(\mathbf{s}; \ell) = V_\ell^{-1} E_s(\mathbf{s}^*) \int d\mathbf{s}' \chi(\mathbf{s} + \mathbf{s}') = E_s(\mathbf{s}^*) \chi(\mathbf{s}; \ell),$$

where  $\mathbf{s}^*$  is a point inside the sphere  $V_\ell$ . Since the volume of the sphere  $V_\ell$  is assumed to be small compared to the size of the sample, the elastic modulus of the solid phase does not vary considerably within  $V_\ell$ . Hence, the approximation  $E_s(\mathbf{s}^*) \approx E_s(\mathbf{s} + \mathbf{s}')$ ,  $\forall \mathbf{s} + \mathbf{s}' \in V_\ell$  is meaningful. Then, in light of Eq. (12) we obtain the approximation  $E_s(\mathbf{s}^*) \approx E_s(\mathbf{s}; \ell)$ .

The mean value of the solid-phase modulus remains invariant under coarse-graining, i.e.  $\mathbb{E}[E_s(\mathbf{s}; \ell)] = \bar{E}_s$ . This follows from Eq. (12) upon permuting the integration and the expectation operator, and applying the definition  $\mathbb{E}[E_s(\mathbf{s} + \mathbf{s}')] = \bar{E}_s$  (cf. second paragraph in Section 2.1.3). Thus, based on Eq. (6), the mean elastic modulus is given to leading order by the following product of mean values:

$$\mathbb{E}[E(\mathbf{s}; \ell)] = \bar{E}_s(1 - \bar{\phi}). \quad (13)$$

The solid-phase elastic modulus variance changes to  $\text{Var}[E_s(\mathbf{s}; \ell)] < \text{Var}[E_s(\mathbf{s})]$ . To estimate this change, we rely again on the proportional effect, which leads to:

$$\frac{\text{Var}[E_s(\mathbf{s}; \ell)]}{\mathbb{E}^2[E_s(\mathbf{s}; \ell)]} = \alpha_\ell \frac{\sigma_\chi^2(\ell)}{\bar{\chi}^2}, \quad (14)$$

where  $\alpha_\ell$  is the coarse-grained coefficient expressing the proportional effect at the local scale.

The local-scale modulus variance,  $\sigma_E^2(\ell) = \text{Var}[E(\mathbf{s}; \ell)]$ , can be expressed to leading order (ignoring terms that involve fluctuation products) as follows:

$$\sigma_E^2(\ell) = \text{Var}[E_s(\mathbf{s}; \ell)] \mathbb{E}^2[\chi(\mathbf{s}; \ell)] + \mathbb{E}^2[E_s(\mathbf{s}; \ell)] \text{Var}[\chi(\mathbf{s}; \ell)].$$

Using the invariance of the coarse-grained mean field, i.e.  $\mathbb{E}[\chi(\mathbf{s}; \ell)] = 1 - \bar{\phi}$ , the invariance of the solid-phase modulus,  $\mathbb{E}[E_s(\mathbf{s}; \ell)] = \bar{E}_s$ , and the phase-field's variance reduction as expressed by Eq. (11), it follows that the variance of the local modulus is given by:

$$\sigma_E^2(\ell) = \text{Var}[E_s(\mathbf{s}; \ell)](1 - \bar{\phi})^2 + g_\ell \bar{E}_s^2(1 - \bar{\phi})\bar{\phi}. \quad (15)$$

Based on Eqs. (13) and (15), the coefficient of variation of the local modulus is given by:

$$\mu_E^2(\ell) = \frac{\sigma_E^2(\ell)}{\mathbb{E}^2[E(\mathbf{s}; \ell)]} = \frac{(g_\ell + \alpha_\ell)\bar{\phi}}{1 - \bar{\phi}} = (g_\ell + \alpha_\ell)\mu_\chi^2. \quad (16)$$

For highly homogeneous ceramic materials the porosity is small, i.e.  $\bar{\phi} < 0.05$ , and  $\mu_E \ll 1$ . Then, low-order (in  $\mu_E$ ) perturbation methods can be used for determining accurately the macroscopic elastic modulus. For porosity values near 0.5, higher-order terms in the expansion become important. However, at  $\bar{\phi} = 1$  the elastic modulus is uniformly equal to zero and thus  $\mu_E$  should equal zero. Yet, at  $\bar{\phi} = 1$  the local modulus coefficient of variation given by (16) tends to infinity in light of Eq. (1). This non-physical result emphasizes that the expansion is valid around the  $\bar{\phi} = 0$  state. In fact, the coefficient of variation is not a meaningful quantity for measuring the variability when the mean value tends to zero.

In conclusion, we assume that at the local scale the elastic modulus can be modeled as a continuum random field. The persistence of the spatial correlations is controlled by the correlation length  $\xi_\ell$ . The mean value of the field is given by Eq. (13) and the variance by Eq. (15). Due to the coarse-graining we expect that the fluctuations of the local modulus are approximately governed by the Gaussian (normal) distribution.<sup>f</sup> The two-point correlation function  $c_E(\mathbf{r})$  governs the spatial distribution of the heterogeneities. Higher-order correlations follow from  $c_E(\mathbf{r})$ , if the local modulus distribution (or its logarithm, in case of a lognormal distribution) is jointly Gaussian.

### 2.3. Macro scale: effective elastic modulus

For most purposes, measurements of the elastic modulus typically represent a single value per each (macroscopic) sample. The values obtained for different samples may differ. Let  $L$  determine the longer dimension of the sample. If  $L$  is large compared to  $\xi_\ell$ , sample-to-sample variations are small (assuming that there

<sup>f</sup> The normal distribution is not formally the best choice, since it allows a finite, albeit extremely small, probability for negative modulus values. A more appropriate distribution is the lognormal distribution. However, the differences between the two distributions become practically negligible as the heterogeneity is reduced (i.e. as the coefficient of variation tends to 0).

are no differences in the sample preparation procedure and that the samples are not damaged). If these ergodic conditions are satisfied, it is meaningful to define an *effective Young's modulus* that represents the elastic modulus of the ceramic.

Let us define by  $\sigma_{ij}(\mathbf{s})$  the *local stress tensor*, and by  $\varepsilon_{kl}(\mathbf{s})$  the *local strain tensor*. Then, assuming uniaxial loading in the direction  $z$ , the macroscopic Young's modulus is given by means of the following ratio:

$$E_{\text{eff}} = \frac{\langle \sigma_{zz} \rangle}{\langle \varepsilon_{zz} \rangle}, \quad (17)$$

where the brackets denote the *spatial average* over the local fluctuations (at each point  $\mathbf{s}$ ) of the strain and stress fields.<sup>g</sup> If the ergodic conditions are satisfied, the stress and strain field averages can be expressed as averages over the probability distribution of the local modulus.

In principle, to determine the average stress and strain fields one needs to solve the force-balance equations [2, p.16]  $\partial_j \sigma_{ij}(\mathbf{s}) + f_i(\mathbf{s}) = 0$ , where  $\partial_j \sigma_{ij}(\mathbf{s})$  denotes the partial derivative of the stress tensor in the  $j$  th direction, and  $f_i$  the component of distributed force density in the  $i$  th direction.<sup>h</sup> The applied load is typically incorporated in the boundary conditions. Using the constitutive stress–strain equations of linear elasticity, the force-balance equation can also be expressed as  $\partial_j C_{ijkl}(\mathbf{s}) \varepsilon_{kl}(\mathbf{s}) + f_i(\mathbf{s}) = 0$ , where  $C_{ijkl}(\mathbf{s})$  is the *fourth-rank stiffness tensor*.<sup>2</sup> This equation can be solved in principle by exact expressions that yield analytical results using approximations (e.g. geometry of non-homogeneous inclusions, truncation of the resulting series) or simplifications (e.g. phases with homogeneous moduli).<sup>18–21</sup> Most approaches focus on the expansion of the stiffness tensor around a homogeneous tensor. The impact of the non-homogeneities is incorporated by the convolution of the correlation functions at various orders with the Green's function of the homogeneous problem. This approach leads to integro-differential equations from which formal expansions can be developed.

Here, we propose an intuitively motivated expression for the effective Young's modulus, which is based on physical grounds. First, we assume that the Young's modulus does not depend on the value of the Poisson's ratio. This assumption is also used in other theories and is validated by numerical experiments.<sup>1,3</sup> Hence, the main parameters that affect the elastic coefficients at the local scale are:  $\mathbb{E}[E(\mathbf{s}; \ell)]$ ,  $\mu_E(\ell)$ , and  $\xi_\ell$ . The correlation function  $c_E(\mathbf{r})$ , is another potential factor. However, if the sample size is adequately large, the exact form of the correlation function (so long as the latter is isotropic) is not crucial. The role of the sample size in upscaling expressions for the related problem of fluid flow in porous media is discussed in<sup>16</sup>. As argued in Section 2.2.2, the key perturbation parameter is the coefficient of variation of the local elastic modulus,  $\mu_E(\ell)$ . Hence, it makes sense to express the effective modulus as a series expansion in

terms of  $\mu_E(\ell)$ . The latter should show up at various orders, corresponding to different orders of non-homogeneities. However, in the weak-heterogeneity limit the impact of the higher orders is comparatively reduced.

Motivated by the above considerations and detailed calculations applying to two-dimensional elastic sheets,<sup>22</sup> we propose the following expression for the perturbation expansion of the effective Young's modulus:

$$E_{\text{eff}} = \mathbb{E}[E(\mathbf{s}; \ell)] \left[ 1 + \sum_{n=1}^{\infty} \mu_E^{2n}(\ell) c_{2n} \right], \quad (18)$$

where  $c_{2n}$  are perturbation coefficients that correspond to the 2  $n$ -th order of the expansion. These coefficients incorporate integrals over the correlation functions and the Green's function of the homogeneous problem, as discussed above. Eq. (18) is an *educated ansatz* for the result obtained by evaluating explicitly the Neumann–Born expansion [23, pp. 470–474] of the effective modulus. The right hand side of (18) is dimensionally correct and yields the expected modulus, i.e.  $E_{\text{eff}} = \bar{E}_s$ , at the limit of a completely homogeneous, zero-porosity ceramic. If the coefficient of variation vanishes, Eq. (18) also gives the expected result, i.e.  $\mathbb{E}[E(\mathbf{s}; \ell)]$ . Eq. (18) contains only the crucial statistical parameters for large samples, as argued in the preceding paragraph.

A brief sketch of the derivation of Eq. (18) follows. In light of Eq. (17), the effective elastic modulus is obtained from solving the macroscopic constitutive relation  $\langle \sigma_{zz} \rangle = E_{\text{eff}} \langle \varepsilon_{zz} \rangle$ . Approximately,<sup>i</sup> it holds that  $\langle \sigma_{zz} \rangle \approx \langle E(\mathbf{s}; \ell) \varepsilon_{zz}(\mathbf{s}) \rangle$ . In view of the constitutive relation, the latter approximation implies that  $\langle E(\mathbf{s}; \ell) \varepsilon_{zz}(\mathbf{s}) \rangle \approx E_{\text{eff}} \langle \varepsilon_{zz} \rangle$ .<sup>j</sup> Evaluation of the average on the left hand side makes use of the decomposition  $E(\mathbf{s}; \ell) = \mathbb{E}[E(\mathbf{s}; \ell)] + E'(\mathbf{s}; \ell)$ , where the mean local modulus  $\mathbb{E}[E(\mathbf{s}; \ell)]$  is given by Eq. (13) and  $E'(\mathbf{s}; \ell)$ , is the fluctuation of the local scale modulus. In addition, the longitudinal strain is expanded as  $\varepsilon_{zz}(\mathbf{s}) = \varepsilon_{zz}^{(0)}(\mathbf{s}) + \sum_{m=1}^{\infty} \mu_E^m(\ell) \varepsilon_{zz}^{(m)}(\mathbf{s})$ , where  $\varepsilon_{zz}^{(0)}(\mathbf{s})$  is the strain of a homogeneous medium with elastic modulus  $\mathbb{E}[E(\mathbf{s}; \ell)]$ , and  $\varepsilon_{zz}^{(m)}(\mathbf{s})$  is the strain perturbation caused by the non-homogeneity of the elastic modulus at order  $m$  (where  $m$  is a positive integer). The perturbations  $\varepsilon_{zz}^{(m)}(\mathbf{s})$  are consequently expressed in terms of the Green's function of the homogeneous problem and the local non-homogeneities of the elastic modulus, using the Neumann–Born series expansion. Finally, the ensemble average  $\langle E(\mathbf{s}; \ell) \varepsilon_{zz}(\mathbf{s}) \rangle$  is evaluated. In the series expansion (18), the perturbation coefficients  $c_{2n}$  involve convolutions of the homogeneous Green's function with the normalized correlation function  $\rho_E(\mathbf{r}) = c_E(\mathbf{r})/\sigma_E^2$ . Since the local modulus variations are Gaussian, odd order terms vanish when the ensemble average  $\langle E(\mathbf{s}; \ell) \varepsilon_{zz}(\mathbf{s}) \rangle$  is calculated. Furthermore, if the macroscopic

<sup>i</sup> That is, if the impact of off-diagonal terms of the stiffness tensor is ignored for the uniaxial loading condition.

<sup>j</sup> In this approximation we ignore the impact on  $\langle \sigma_{zz} \rangle$  of strain non-homogeneities that arise from the non-loading directions. It is reasonable to expect that these have a much smaller magnitude than non-homogeneities in the loading direction; the off-loading strain non-homogeneities couple to the off-diagonal elements of the stiffness tensor, thereby further reducing their impact.

<sup>g</sup> For example,  $\langle \sigma_{zz} \rangle = 1/|V_S| \int_{V_S} \sigma_{zz}(\mathbf{s}) \, ds$ , where  $\int_{V_S} ds$  denotes the volume integral over the sample and  $|V_S|$  the sample volume.

<sup>h</sup> Summation is implied over repeated indices,  $j$  on the same side of the equation.

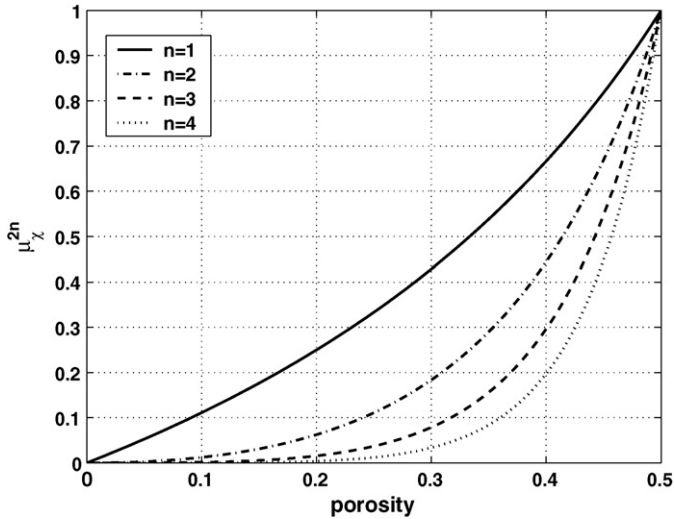


Fig. 1. Comparison of the terms  $\mu_E^{2n}(\ell)$  for different values of  $n$ .

scale is large,  $L \gg \xi_\ell$ , the coefficients are not very sensitive on the exact form of  $\rho_E(\mathbf{r})$ .

According to Eq. (16), if we set  $\alpha_\ell + g_\ell = 1$  then  $\mu_E^{2n}(\ell) = \mu_\chi^{2n}$ . The terms  $\mu_\chi^{2n}$ , for  $n = 1, 2, 3, 4$ , are compared in Fig. 1. For low porosity values only the first term is significant, while at  $\bar{\phi} = 1$  all the terms converge to 1. The contribution of the terms with larger  $n$  is further reduced compared to the terms with lower  $n$  if  $\alpha_\ell + g_\ell < 1$ .

If we truncate the expansion at  $n = 2$  and use Eq. (13) for the mean local modulus, we obtain the following estimator  $\hat{E}_{\text{eff}} \approx E_{\text{eff}}$ :

$$\hat{E}_{\text{eff}} = \bar{E}_s (1 - \bar{\phi}) [1 + c_2 \mu_E^2(\ell) + c_4 \mu_E^4(\ell)]. \quad (19)$$

Further, in light of (16), this is expressed as follows:

$$\hat{E}_{\text{eff}} = \bar{E}_s (1 - \bar{\phi}) (1 - \beta_1 \mu_\chi^2 + \beta_2 \mu_\chi^4), \quad (20)$$

where  $\beta_1 = -c_2(\alpha_\ell + g_\ell)$  and  $\beta_2 = c_4(\alpha_\ell + g_\ell)^2$  are positive empirical coefficients. The signs of the coefficients  $\beta_1$  and  $\beta_2$  are motivated by the close connection between the force balance equation and the equation of fluid flow in a porous medium (in fact, they are equivalent in one dimension). In the latter case, the non-homogeneities lead to an alternating series for the effective permeability.<sup>16</sup> Intuitively, we can visualize this effect as the fluctuations at each perturbation order tending to cancel the impact of the preceding order: the first-order correction tends to reduce the magnitude of the uniform elastic modulus, the second-order correction tends to reduce (in magnitude) the impact of the first-order correction, etc. The choice of the signs<sup>k</sup> is validated by the analysis of experimental elastic moduli, given in Section 3 below, that results consistently in positive values for the coefficients  $\beta_1, \beta_2$ .

Eq. (1) can be used to express  $\mu_\chi^2$  in terms of  $\bar{\phi}$ . Then, expanding the resulting expression into a Taylor series around  $\bar{\phi} = 0$ , we obtain the following series for the effective modulus estimator:

$$\hat{E}_{\text{eff}} = \bar{E}_s \left[ 1 - (1 + \beta_1) \bar{\phi} + \beta_2 \sum_{n=2}^{\infty} \bar{\phi}^n \right]. \quad (21)$$

Hence,  $\hat{E}_{\text{eff}}$  can be viewed as a polynomial expansion in  $\bar{\phi}$  in terms of just two positive empirical coefficients. The coefficients  $\beta_1$  and  $\beta_2$  are related to the first two derivatives of the  $\hat{E}_{\text{eff}}$  versus  $\bar{\phi}$  curve at the origin, since  $d\hat{E}_{\text{eff}}/d\bar{\phi}|_{\bar{\phi}=0} = -(1 + \beta_1)$ , while  $d^2\hat{E}_{\text{eff}}/d\bar{\phi}^2|_{\bar{\phi}=0} = 2\beta_2$ .

#### 2.4. On the physical significance of the empirical coefficients

Various models connecting the Young's modulus to porosity exist in the literature. Certain models take advantage of direct connections with particular features of the microstructure. For example, in the model by Wagh et al.<sup>24</sup> an empirical exponent is linked to the tortuosity of the ceramic's structure. A different model by Rice<sup>25</sup> addresses the connection between the elastic modulus and minimum solid areas related to the connectivity of the pore space. Models by Jernot et al.<sup>26</sup> and Arató et al.<sup>27</sup> emphasize the dependence of the modulus on the coordination number of the grains. The model of Phani and Niyogi<sup>7</sup> employs the concept of critical porosity in the sense of percolation theory. The model of Roberts and Garboczi<sup>1</sup> investigates, using synthetic media, the impact of the microstructure created by overlapping spheres, spherical pores, and ellipsoidal pores.

In the model presented herein, the emphasis is placed on the correlation functions of the phase field. The empirical coefficients, as argued above, involve convolutions of the two-point and four-point phase field correlation functions. It is well accepted to date that the stochastic representation of porous microstructures is possible in terms of phase-field correlation functions.<sup>4</sup> In particular, the first derivative of the phase-field correlation function (calculated at zero distance) is proportional to the specific (i.e. per unit volume) interfacial area of the pore space to solid-matrix interface,<sup>28</sup> [4, p. 37]. If the pore space is formed by identical, three-dimensional impenetrable spheres, the second derivative of the correlation function is proportional to the mean coordination number [4, p. 38]. Various such relations between the microstructural properties and the correlation functions exist, c.f. [4, Chap. 2]. In addition, studies on synthetic media<sup>29</sup> show a clear dependence of the two-point correlation function on the shape and spatial arrangement of the pores. Capitalizing on these relations, various stochastic reconstruction methods of the microstructure have been proposed.<sup>9–11,30</sup> Such methods accomplish three-dimensional reconstructions of porous media using statistical information about the microstructure; this information is derived from tomographic two-dimensional images<sup>30</sup> obtained by means of invasive<sup>9</sup> or non-invasive methods.<sup>31</sup>

<sup>k</sup> The nature of the signs (+ or -) is not linked to the dimensionality, but rather to the  $\partial_j$  partial derivative operator in the force balance equation: the term of  $O(\mu_E^2(\ell))$  in the expansion involves the pair  $\partial_{j_1} \partial_{j_2}$ , which in the spectral domain is proportional to  $-k_{j_1} k_{j_2}$ ,  $\mathbf{k}$  being the wavevector.

### 2.5. Empirical lower and upper bounds on the Young's modulus

Note that the dependence of the effective modulus, Eq. (20), on the parameters  $\beta_1$  and  $\beta_2$  is monotonic:  $\hat{E}_{\text{eff}}$  is a decreasing function of  $\beta_1$  and an increasing function of  $\beta_2$ . The values of  $\beta_1$  and  $\beta_2$  are expected to differ between ceramics, depending on the composition, the details of the microstructure and the processing conditions. Hence, we can formulate empirical lower  $E_{\text{eff}}^{(l)}$  and upper  $E_{\text{eff}}^{(u)}$  bounds as follows:

$$E_{\text{eff}}^{(l)} = \bar{E}_s(1 - \bar{\phi})(1 - \beta_{1,\text{max}} \mu_\chi^2 + \beta_{2,\text{min}} \mu_\chi^4), \quad (22)$$

$$E_{\text{eff}}^{(u)} = \bar{E}_s(1 - \bar{\phi})(1 - \beta_{1,\text{min}} \mu_\chi^2 + \beta_{2,\text{max}} \mu_\chi^4). \quad (23)$$

The values  $\beta_{p,\text{min}}$  and  $\beta_{p,\text{max}}$  ( $p = 1, 2$ ) are empirical coefficients determined from the available data sets. Hence, the bounds defined by Eqs. (22) and (23) do not have the rigor of the various mathematical (e.g. two-point, three-point, variational) bounds on elastic moduli.<sup>4</sup> However, they can provide useful estimators of the expected elastic modulus if only porosity information is available. These empirical bounds can be updated as measurements on new materials become available, leading to improved estimates for the range of the coefficients  $\beta_1$  and  $\beta_2$ .

Table 1

Estimates of the model parameters  $\bar{E}_s$ ,  $\beta_1$ , and  $\beta_2$  for various ceramic materials

Material	$\beta_1$	$\delta\beta_1$	$\beta_2$	$\delta\beta_2$	$\bar{E}_s$ (GPa)
Al <sub>2</sub> O <sub>3</sub>	1.66	±0.27	1.51	±0.49	377.04
B <sub>4</sub> C	4.80	±na	1.50	±na	462.27
Lu <sub>2</sub> O <sub>3</sub>	1.56	±0.36	0.69	±0.82	197.17
Si <sub>3</sub> N <sub>4</sub>	1.77	±0.46	1.36	±1.05	294.91
ThO <sub>2</sub>	1.76	±0.04	0.82	±1.05	259.21
ZnO	1.52	±0.76	0.67	±0.31	121.54
MgAl <sub>2</sub> O <sub>4</sub>	1.77	±0.17	1.05	±0.33	280.34
ZrO <sub>2x</sub> Y <sub>2</sub> O <sub>3</sub>	1.95	±0.65	1.69	±1.18	214.29

The parameters  $\delta\beta_1$  and  $\delta\beta_2$  represent the half-width of the 95% confidence intervals. The symbol "na" means that the half-width estimate is not available.

### 3. Comparison of effective modulus with experimental data

For many ceramic materials of interest (advanced, engineering, functional and some traditional ceramics, e.g. porcelain) the porosity is low (less than 5%), about 0.5% of which may correspond to disconnected pores. Traditional ceramic materials have higher porosity: in refractories the porosity is about 20% to provide resistance to thermal shocks; wall tiles have porosities in the range 10–20% as a result of the production process (fast firing cycle and non-equilibrium phases) and due to the fact that lighter tiles are recommended for walls; clay derived bricks have porosi-

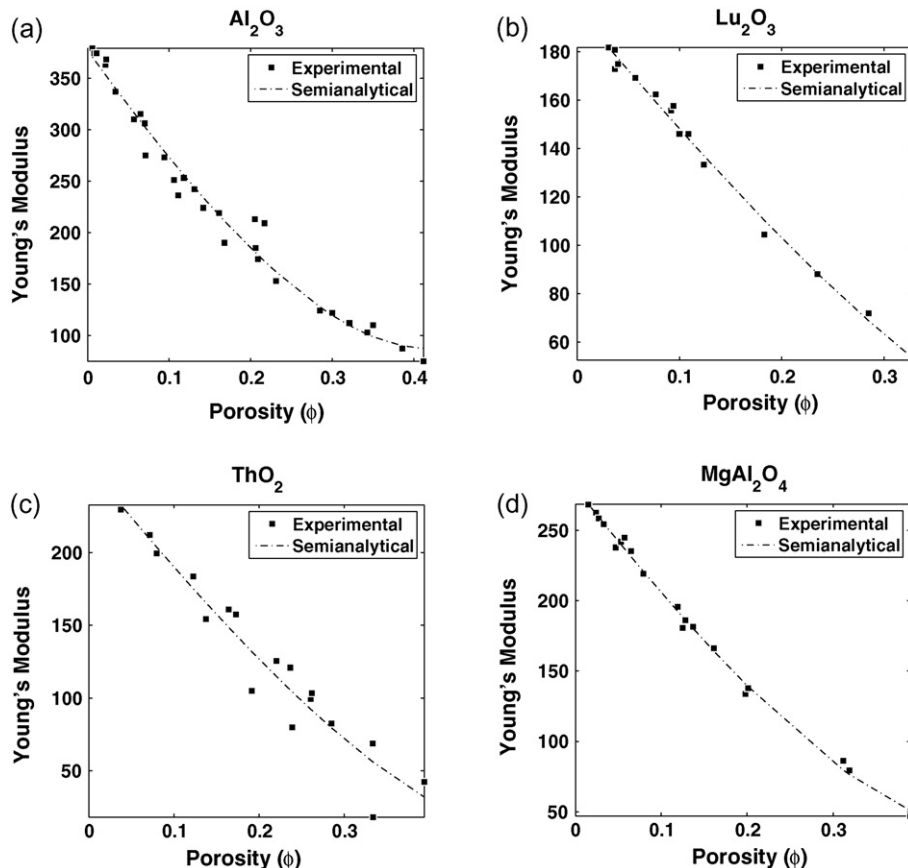


Fig. 2. Young's modulus (in GPa) of Al<sub>2</sub>O<sub>3</sub>(a), Lu<sub>2</sub>O<sub>3</sub>(b), ThO<sub>2</sub> (c), and MgAl<sub>2</sub>O<sub>4</sub> (d) ceramics: experimental data and curves fitted to the semi-analytical expression (20).

ties around 40% to obtain reduced thermal conductivity, while for some refractory insulation bricks the porosity is in the range 40–50%. Hence, the model is applicable to various ceramic materials. For the ceramic materials investigated here the porosity takes values up to 40%. The experimental data of Young's modulus versus porosity were downloaded from the database of the National Institute of Standards and Technology.<sup>41</sup> These values were obtained from the investigations reported in<sup>32–40</sup>.

The data are fitted to the analytical relation (20). The estimates for the three model parameters,  $\bar{E}_s$ ,  $\beta_1$ , and  $\beta_2$ , are presented in Table 1. The half-widths  $\delta\beta_1$ ,  $\delta\beta_2$ , of the 95% confidence interval for the parameters  $\beta_p$  ( $p = 1, 2$ ) are also included in Table 1 (with the exception of  $B_4C$ , due to the small number of samples in this data set).

The experimental data are plotted and compared to the Eq. (20) in Figs. 2 and 3. The data and the analytical expression are in good agreement, even for the higher porosities in the range 0.30–0.40.

With the exception of  $B_4C$ , the parameter  $\beta_1$  takes values in the range [1.52–1.95], while  $\beta_2$  takes values in the range [0.67–1.51]. We attribute the observed variations to differences in the microstructure that are not captured explicitly by the model. The values for each coefficient are of similar magnitude (around one), indicating that the proposed expansion (20) has a physical basis. Also,  $\beta_2/\beta_1 < 1$  for all the cases studied. This property is in agreement with the expectation for

a convergent series expansion. The linear correlation coefficient of  $\beta_1$  and  $\beta_2$  is 73%, suggesting that the changes in the magnitude of the two coefficients are correlated. This correlation supports the argument that they are both related to the microstructure.

#### 4. Discussion

A semi-analytical expression for the effective Young's modulus of ceramics was presented. The expression is derived from a conceptual model that relates the microstructure to the elastic properties. The upscaling procedure used in this paper is based on the phase-field representation at the micro scale, leading to a continuum random field for the elastic variations at the local scale, and to an effective modulus at the macro (measurement) scale. The resulting expression is not completely determined, since the force balance equations are not explicitly solved. To compensate for the indeterminacy, the empirical coefficients  $\beta_1$  and  $\beta_2$  are used in the perturbation expansion of the effective modulus.

The physical insight brought forth by the upscaling process is that the macroscopic elastic modulus is controlled by the coefficient of variation of the local modulus variations. Using the phase field representation the latter can be expressed by means of Eq. (1) as a nonlinear function of the volume fraction of porosity.

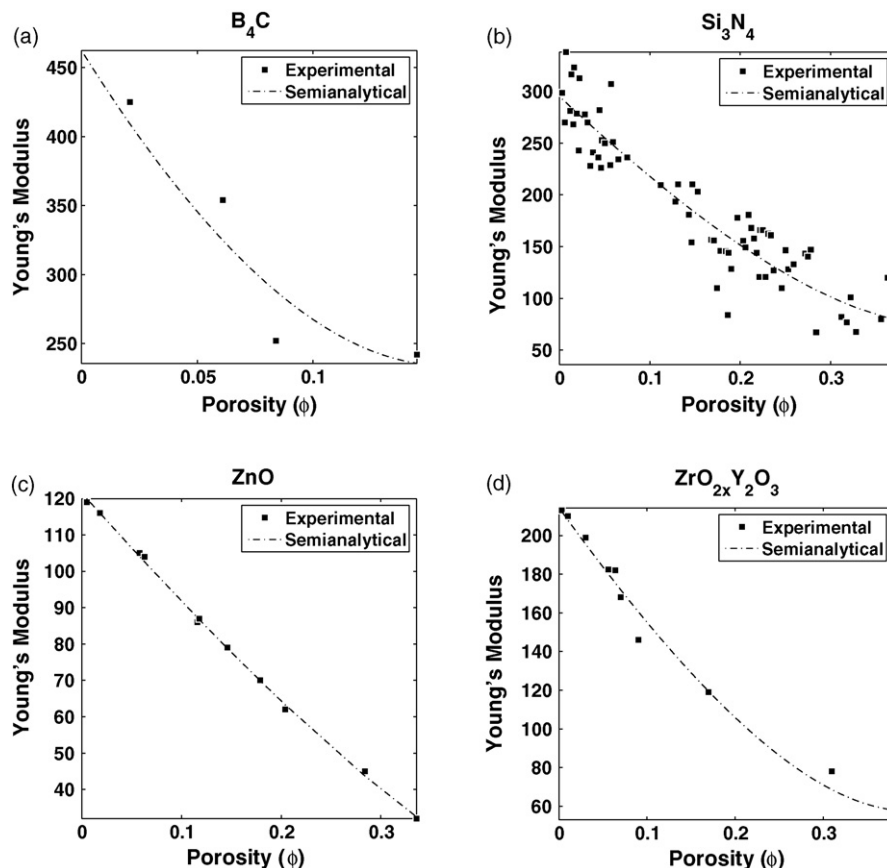


Fig. 3. Young's modulus (in GPa) of  $B_4C$  (a),  $Si_3N_4$  (b),  $ZnO$  (c), and  $ZrO_{2-x}Y_2O_3$  (d) ceramics: experimental data and curves fitted to the semi-analytical expression (20).



In spite of the approximations employed, very good agreement with available experimental data is obtained. Deviations of the experimental results from the semi-analytical expression may be attributed to non-ergodic (sample-to-sample) fluctuations, which occur if the sample size is not large compared to the correlation length  $\xi_\ell$ .

The argument used for the Young's modulus can not be extended to the estimation of the Poisson's ratio, which relates transverse and longitudinal strain. Hence, a detailed solution of the stress-strain equations is necessary to derive a physically meaningful expression for  $\nu$ .

As shown in Table 1, the two empirical coefficients  $\beta_1$  and  $\beta_2$  in (20) depend on the specific material. This result implies that a simple porosity dependence can not capture the variations of the Young's modulus. For isotropic materials the bulk modulus,  $K$ , can be considered independent of microstructural details, in contrast with the shear modulus,  $G$  [4, pp. 541–546]. Since  $G = E/(2(1 + \nu))$  and  $K = E/(d[1 + \nu(1 - d)])$  (where  $d$  denotes the dimensionality,) the Young's modulus is expected to depend on the specific microstructure. This observation is in agreement with the conclusion of the present study.

## 5. Conclusions

A new equation for the estimation of the effective Young's modulus in isotropic ceramic materials as a function of the volume fraction of porosity is proposed. It is shown that the estimator accurately represents the porosity dependence of experimental data. Like the Phani–Niyogi relation, the proposed estimator involves three empirical parameters: the solid phase modulus and two perturbation coefficients. These parameters depend on the ceramic's composition and possibly the processing methods used. The empirical upper and lower bounds (22) and (23) provide a different means of estimating the Young's modulus of a ceramic material, if only the porosity and the value of the solid-phase modulus are available.

## Acknowledgments

Research supported by the European Union (FP6) grant “Super High Energy Milling in the Production of Hard Alloys, Ceramic and Composite Materials (Activation),” contract no. NMP2-CT-2004-505885-1. We would like to acknowledge Prof. M. Sopicka-Lizer (Silesian Technical University, Poland) and Prof. Z. Agioutantis (Technical University of Crete) for their suggestions, as well an anonymous referee for helpful comments.

## References

1. Roberts, A. P. and Garboczi, E. J., Elastic properties of model porous ceramics. *J. Am. Ceram. Soc.*, 2000, **83**, 3041–3048.
2. Landau, L. P. and Lifshitz, I. M., *Theory of Elasticity*. Pergamon Press, New York, 1970.
3. Munro, R. J., Analytical representations of elastic moduli data with simultaneous dependence on temperature and porosity. *J. Res. Natl. Stand. Technol.*, 2004, **109**, 497–503.
4. Torquato, S., *Random Heterogeneous Materials*. Springer, New York, 2002.
5. Reddy, R. R., Muralidhar, M., Babu, V. H. and Venugopal, P., The relationship between the porosity and elastic moduli of the Bi-Pb-2212 high-Tc superconductor. *Supercond. Sci. Technol.*, 1995, **8**, 101–107.
6. Pabst, W., Gregorová, E. and Tichá, G., Elasticity of porous ceramics: a critical study of modulus-porosity relations. *J. Eur. Cer. Soc.*, 2005, **26**, 1085–1097.
7. Phani, K. K. and Niyogi, S. K., Young's modulus of porous brittle solids. *J. Mater. Sci.*, 1987, **22**, 257–263.
8. Deng, M. and Dodson, C. T. J., *Paper-An Engineered Stochastic Structure*. TAPPI Press, Atlanta, 1994.
9. Adler, P. M., Jacquin, C. G. and Quiblier, J., Flow in simulated porous media. *Int. J. Multiphase Flow*, 1990, **16**(44), 691–712.
10. Yeong, C. L. Y. and Torquato, S., Reconstructing random media. *Phys. Rev. E*, 1998, **57**(1), 495–506.
11. Yeong, C. L. Y. and Torquato, S., Reconstructing random media. II. Three-dimensional media from two-dimensional cuts. *Phys. Rev. E*, 1998, **58**(1), 224–233.
12. Hornung, U., *Homogenization and Porous Media*. Springer, 1997.
13. Hilfer, R., Local porosity theory and stochastic reconstruction for porous media. In *Statistical Physics and Spatial Statistics. The Art of Analyzing and Modeling Spatial Structures and Pattern Formation*, ed. K. R. Mecke and D. Stoyan. Lecture Notes in Physics, Vol. 554, pp. 203–241.
14. Hilfer, R., Local porosity theory for flow in porous media. *Phys. Rev. B*, 2002, **45**(13), 7115–7121.
15. Bouchaud, J-P. and Georges, A., Anomalous diffusion in disordered media: statistical mechanics, models and physical applications. *Phys. Rep.*, 1990, **195**, 127–293.
16. Hristopulos, D. T., Renormalization group methods in subsurface hydrology: overview and applications in hydraulic conductivity upscaling. *Adv. Water Resour.*, 2003, **26**(12), 1279–1308.
17. Whittaker, E. T. and Watson, G. N., *A Course of Modern Analysis (4th ed.)*. Cambridge University Press, New York, 1992.
18. Shatalov, G. A., Effective characteristics of isotropic composites as a multiple-body problem. *Mech. Composite Mater.*, 1985, **21**(1), 33–41.
19. Hirsekrorn, S., Elastic properties of polycrystals: a review. *Textures Microstruct.*, 1990, **12**, 1–14.
20. Ju, J. W. and Chen, T. M., Effective elastic moduli of two-phase composites containing randomly dispersed spherical inhomogeneities. *Acta Mech.*, 1994, **103**, 123–144.
21. Torquato, S., Exact expression for the effective elastic tensor of disordered composites. *Phys. Rev. Lett.*, 1997, **79**(4), 681–684.
22. Hristopulos, D. T. and Uesaka, T., Structural disorder effects on the tensile strength distribution of heterogeneous brittle materials with emphasis on fiber networks. *Phys. Rev. B*, 2004, **70**(6), art.no. 064108.
23. Byron, F. W. and Fuller Jr, R. W., *Mathematics of Classical and Quantum Physics*. Dover, NY, 1992.
24. Rice, M. W., Evaluation and extension of physical property-porosity models based on minimum solid area. *J. Mater. Sci.*, 1996, **31**, 102–118.
25. Wagh, A. S., Poeppel, R. B. and Singh, J. P., Open pore description of mechanical properties of ceramics. *J. Mater. Sci.*, 1991, **26**, 3862–3868.
26. Jernot, J. P., Coster, M. and Chermant, F., A model to describe the elastic modulus of sintered materials. *Phys. Stat. Sol. A*, 1982, **72**, 142–148.
27. Arato, P., Besenyei, E., Kele, A. and Weber, F., Mechanical properties in the initial stage of sintering. *J. Mater. Sci.*, 1995, **30**, 1863–1871.
28. Berryman, J. G., Measurement of spatial correlation functions using image processing techniques. *J. Appl. Phys.*, 1985, **57**, 2374–2384.
29. Braginsky, L., Shklover, V., Witz and Bossmann, H-P., Thermal conductivity of porous structures. *Phys. Rev. B*, 2007, **75**, 094301.
30. Quiblier, J. A., A new three-dimensional modeling technique for studying porous media. *J. Colloid Interface Sci.*, 1984, **98**, 84–102.
31. Mukherjee, P. P. and Wang, C-Y., Stochastic microstructure reconstruction and direct numerical simulation of the PEFC catalyst layer. *J. Electrochem. Soc.*, 2006, **153**, A840–A849.
32. Knudsen, F. P., Effect of porosity on Young modulus of alumina. *J. Am. Ceram. Soc.*, 1962, **45**, 94–95.

33. Hunter, O. and Graddy Jr, G. E., Porosity dependence of elastic properties of polycrystalline cubic  $\text{Lu}_2\text{O}_3$ . *J. Am. Ceram. Soc.*, 1976, **59**, 82.
34. Martin, L. P., Dadon, D. and Rosen, M., Evaluation of ultrasonically determined elasticity-porosity relations in zinc oxide. *J. Am. Ceram. Soc.*, 1996, **79**, 1281–1289.
35. Spinner, S., Knudsen, F. P. and Stone, L., Elastic-constant porosity relations for polycrystalline thoria. *J. Res. Natl. Stand. Technol.*, 1963, **67C**, 39–46.
36. Wu, C. C. and Rice, R. W., Porosity dependence of wear and other mechanical properties of fine grain  $\text{Al}_2\text{O}_3$  and  $\text{B}_4\text{C}$ . *Ceram. Eng. Sci. Proc.*, 1985, **6**, 977–993.
37. Luo, J. and Stevens, R., Porosity-dependence of elastic moduli and hardness of 3y-tzp ceramics. *Ceram. Internat*, 1999, **25**, 281–286.
38. Datta, S. K., Mukhopadhyay, A. K. and Chakraborty, D., Young's modulus-porosity relationships for  $\text{Si}_3\text{N}_4$  ceramics - a critical evaluation. *Am. Ceram. Soc. Bull.*, 1989, **68**, 2098–2102.
39. Porter, D. F., Reed, J. S. and Lewis, D., Elastic moduli of refractory spinels. *J. Am. Ceram. Soc.*, 1977, **60**, 345–349.
40. Soga, N. and Schreiber, E., Porosity dependence of sound velocity and poisson's ratio for polycrystalline MgO determined by resonant sphere method. *J. Am. Ceram. Soc.*, 1968, **51**, 465–466.
41. NIST Structural Ceramics Database, SRD Database Number 30, April 2003. Available at: <http://www.ceramics.nist.gov>.